PACS numbers: 71.45.Lr, 72.30.+q, 73.20.Mf

**V. V. Popov**

Kotelnikov Institute of Radio Engineering and Electronics (Saratov Branch) RAS
410019, Saratov, Russia
E-mail: popov@soire.renet.ru

# PLASMONIC DEVICES FOR DETECTION OF TERAHERTZ RADIATION [*]

Physics of plasma oscillations and basic principles of plasmonic detection of terahertz radiation in FET structures with two-dimensional electron channels are discussed. Plasmonic devices are practically attractive because they are extremely fast and electrically tunable through the entire terahertz frequency band by changing electric potentials at metal contacts of the device.

*Keywords*: two-dimensional electron gas, plasmons, terahertz radiation, detection, generation, field-effect transistor.

**В. В. Попов**

## ПЛАЗМОННЫЕ УСТРОЙСТВА ДЛЯ ДЕТЕКТИРОВАНИЯ ТЕРАГЕРЦЕВОГО ИЗЛУЧЕНИЯ

Обсуждаются физика плазменных колебаний и основные принципы плазмонного детектирования терагерцового излучения в структурах полевых транзисторов с двумерными электронными каналами. Плазмонные устройства имеют практическую привлекательность благодаря тому, что они обладают высоким быстродействием и поддаются электрической перестройке во всем терагерцовом диапазоне посредством изменения электрических потенциалов на металлических контактах устройства.

*Ключевые слова*: двумерный электронный газ, плазмоны, терагерцевое излучение, детектирование, генерация, полевой транзистор.

## Introduction

Terahertz (THz) plasmonics is a newly emerging field of THz physics and technology studying the processes of detection and generation of THz radiation by using plasma oscillations (plasmons) in semiconductor microdevices. Terahertz response of semiconductor microdevices with two-dimensional (2D) electron channels such as the field-effect transistors (FETs) and akin devices is strongly affected by plasma oscillations exited in the device channel. This phenomenon can be used for the detection, frequency multiplication and generation of THz radiation [1-4] as well as for THz imaging [5]. Plasmonic devices are practically attractive because they are extremely fast, electrically tunable through the entire THz frequency band by changing electric potentials at metal contacts of the device, and exhibit sub-THz-wavelength response (which is important for THz imaging and THz near-field microscopy). The latest experimental studies show that plasmonic THz detectors demonstrate the responsivity exceeding 100 V/W along with the great signal transmission speed up to $10^9$ cm/s [6] and deeply sub-THz-wavelength spatial resolution. In this paper, the physics of plasma oscillations and basic principles of plasmonic detection of THz radiation in FET structures with 2D electron channels are discussed.

## Plasmon dispersion

In a broad sense, the plasmons are the oscillations of free electric carriers subject to restor-

[*] The author acknowledges the financial support by the Russian Academy of Sciences Program “Fundamentals of Nanotechnologies and Nanomaterials” and by the Russian Foundation for Basic Research (Grants 09-02-00395 and 10-02-93120).

ing Coulomb force in various types (gaseous, metallic or semiconductor) of the plasma. Non-uniform electric currents involved in the plasma oscillations lead to the electric charge separation in the plasma. Plasma oscillations in 2D electron system in semiconductor heterostructures are termed the 2D plasmons. Two different types of plasma oscillations can exist in a FET-like device with 2D electron channel (see Fig. 1). They are plasma oscillations excited in either gated or ungated regions of the electron channel. The dispersion relation for gated plasma oscillation in an infinite 2D electron sheet screened by infinitely wide perfectly conductive gate plane (with neglect of the electron scattering in 2D electron system) is [7]

$$\bar{\omega}_p^2 = \frac{e^2 N}{m^* \varepsilon_0 \left[ \varepsilon_1 + \varepsilon_2 \coth(qd) \right]} q, \qquad (1)$$

where $\bar{\omega}_p$ and $q$ are the frequency and the wavevector of plasma wave, respectively, $N$ is the areal electron density in 2D electron system, $d$ is the gate-to-channel separation, $\varepsilon_0$ is the dielectric permittivity of vacuum, $\varepsilon_1$ and $\varepsilon_2$ are the dielectric constants of surrounding materials below and above 2D electron channel (substrate and barrier materials, respectively), $e$ and $m^*$ are the charge and effective mass of electron, respectively. If the gate plane is close enough to the electron channel so that $qd << 1$, Eq. (1) yields

$$\bar{\omega}_p = q \sqrt{\frac{e^2 N d}{m^* \varepsilon_0 \varepsilon_2}}, \qquad (2)$$

which means that the plasma waves in the gated region of the channel have frequency-independent phase velocity $s = \bar{\omega}_p / q$. The value of the wavevector of the gated plasmons is quantized as $q = n\pi/l$ where $l$ is the length of the gate with $n$ being an integer. However, in a real FET with finite width of the gate finger (which is called the gate length according to common FET terminology), the plasmon modes with even indexes $n$ can not be excited by THz radiation under the gate contact with symmetric boundary conditions at the gate edges (because of zero net dipole moment of such modes). The plasma wave dispersion described by Eq. (2) is similar to that of gravitational waves on the surface of liquid in a shallow basin. Thus, this particular type of plasma waves is occasionally referred to as the "shallow-water plasmons" [8]. The gated plasmons may be also referred to as the "acoustic plasmons" since their linear dispersion, Eq. (2), is similar to that of the acoustic waves. If $d << l$, the areal electron density in the gated region of the channel can be related to the gate voltage by the parallel plate capacitor formula $N = \varepsilon_0 \varepsilon_2 U_0 / ed$, where $U_0 = U_g - U_{th}$ is the difference between the gate voltage $U_g$ and the channel depletion threshold voltage $U_{th}$ Then Eq. (2) acquires a simple form [1]

$$\bar{\omega}_p = q \sqrt{\frac{eU_0}{m^*}} \qquad (3)$$

with the plasmon phase velocity $s = \sqrt{eU_0 / m^*}$.

Plasma oscillations of the other type can be excited in the ungated regions of the channel. The dispersion relation for this kind of plasma waves is [9, 10]

$$\underline{\omega}_p^2 = \frac{e^2 N}{m^* \varepsilon_0 (\varepsilon_1 + \varepsilon_2)} q. \qquad (4)$$

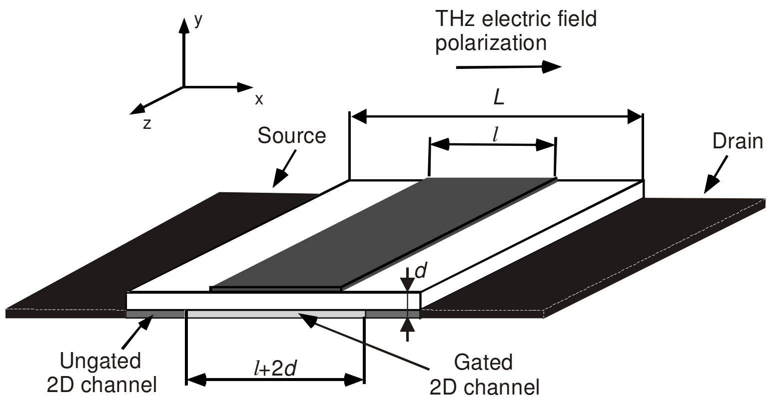


Fig. 1. Schematic of the field-effect transistor structure with 2D electron channel

The value of wavevector $q$ of the ungated plasmons is quantized according to the length of ungated portion of the electron channel. The dispersion described by Eq. (4) is similar to that of gravitational waves on the surface of liquid in a deep basin. Thus, this type of plasma waves are occasionally referred to as the "deep-water plasmons" [11].

Plasmon modes excited under the gate contact (gated plasmons) are more attractive for practical applications because their frequencies can be effectively tuned by varying the gate voltage. Simple estimations performed by using Eq. (2) for typical parameters of FET heterostructure show that the frequency of the fundamental plasmon mode ($n = 1$) exceeds 5 THz if the gate length is shorter than 200 nm. Unfortunately, the gated plasmons in a single-gate FET are weakly coupled to THz radiation [12] because: (i) the gated plasmons are strongly screened by the metal gate contact, (ii) they have a vanishingly small net dipole moment due to their acoustic nature (in this mode, electrons oscillate out-of-phase in the gate contact and in the channel under the gate, which results in vanishingly small net lateral dipole moment), and (iii) gated plasmons strongly leak into ungated access regions of the channel.

Conventional tool for exciting the plasmon modes in 2D electron channel is the metal grating-gate coupler [13, 14] (see Fig. 2). The plasmon dispersion in the grating-gate FET is close to that described by Eq. (1) if the grating finger occupies a considerable part of the grating-gate period. The physics of excitation of plasmon oscillations in a grating-gate FET structure by the incident THz wave can be explained as following. Terahertz electromagnetic wave (with polarization of the electric field across the grating-gate fingers) incident upon the grating gate excites diffracted electromagnetic fields with in-plane wave vectors $q = 2\pi p/L$ ($p$ = 0, ±1, ±2, ±3, …), where $L$ is the grating-gate period. Diffracted electromagnetic waves with $p = 0$ are nothing but the reflected and transmitted waves traveling away from the structure. For a short-period structure $2\pi/L \gg k_0$, where $k_0 = 2\pi/\lambda_0$ with $\lambda_0$ being the THz wavelength, all diffracted electromagnetic fields with $p \neq 0$ are the evanescent fields decaying away from the structure. These evanescent electric fields excite plasmon modes with wavevectors $q = 2\pi p/L$ in 2D electron channel when the frequency of the incident THz wave coincides with the frequency of a respective plasmon mode. Strictly speaking, the field distribution over the period of the structure contains all Fourier-harmonics of the electric field having different wave vectors $q = 2\pi p/L$ for each plasmon mode. However, the $p$th Fourier-harmonic, typically, dominates at the $p$th plasmon resonance frequency determined by Eq. (1) with $q = 2\pi p/L$. For the grating gate with a symmetric unit cell, the Fourier-harmonics of the electric field traveling in the opposite directions (i.e., having the wave vectors of the opposite signs) have equal amplitudes, which means that a standing plasma wave is excited in the structure with a symmetric unit cell. A grating coupler with narrow slits between the metal gate fingers is needed for effective exciting the higher-order plasmon resonances [14] (see Fig. 3) because the narrower slits generate stronger Fourier harmonics of the incident THz electric field.

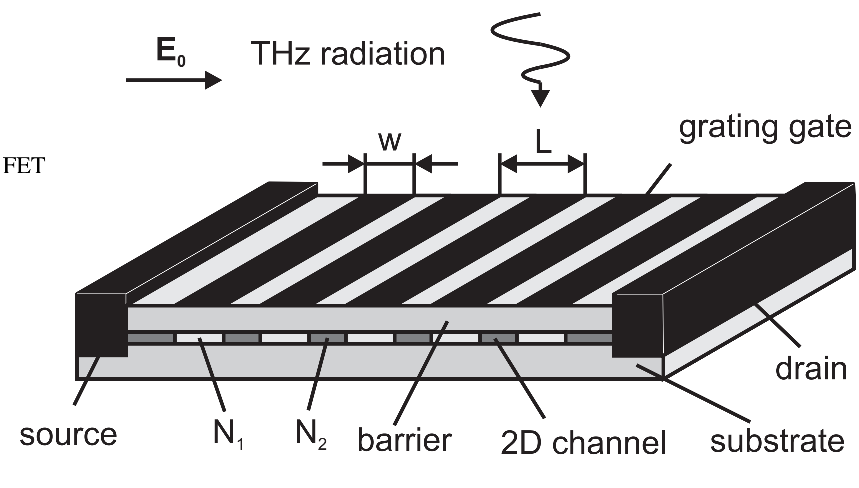


Fig. 2. Schematic view of the FET structure with a grating gate

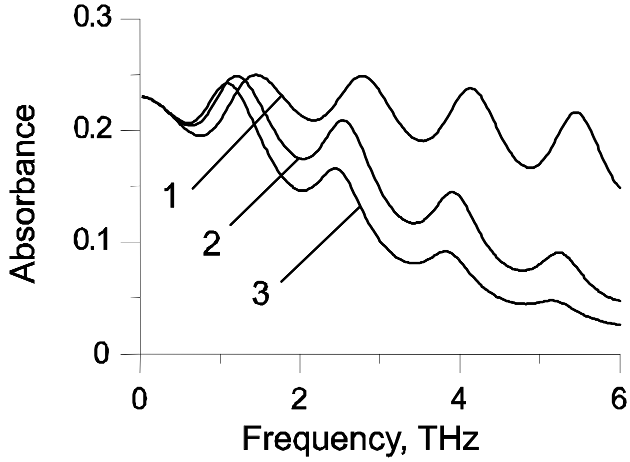


Fig. 3. Calculated absorption spectra of AlGaN/GaN grating-gate FET structure with l-μm-wide grating-gate fingers for three different slit widths: 0.1 μ*m* (curve 1), 0.3 μm (curve 2) and 0.5 μm (curve 3) at room temperature [14]

## Plasmon nonlinearities and terahertz detection

For relatively dense 2D electron plasma, the plasmon dynamics can be described by the hydrodynamic equations for 2D electron fluid [1]

$$\frac{\partial V(x,t)}{\partial t}+V(x,t)\frac{\partial V(x,t)}{\partial x}+ +\frac{V(x,t)}{\tau}+\frac{e}{m^*}E(x,t)=0, \quad (5)$$

$$e\frac{\partial}{\partial t}N(x,t)-\frac{\partial}{\partial x}j(x,t)=0, \quad (6)$$

where $E(x,t)$ is the in-plane electric field depending on the time $t$ and coordinate $x$ in 2D electron system, $\tau$ is the electron momentum relaxation time due to electron scattering in 2D system, $j(x,t)=-eN(x,t)V(x,t)$ is the density of induced electric current, $N(x,t)$ and $V(x,t)$ are hydrodynamic electron density and velocity in 2D electron channel respectively. There are two different nonlinear terms in the system Eqs. (5) and (6): the second term in the Euler equation, Eq. (5), describing the nonlinear electron convection in 2D electron fluid and the product $N(x,t)V(x,t)$ defining the current density in the continuity equation Eq. (6). Time average of the nonlinear current yields the detection signal. It should be noted that either of the two nonlinear terms vanishes in the case of uniform oscillating currents flowing in 2D electron system. Hence, those nonlinearities are related to non-uniform currents inherent in the plasma oscillations. In principle, the both nonlinear terms can contribute to the detection signal depending on the geometry of the structure. However, for symmetry reasons, the detection response must be zero in 2D electron channel with identical boundary conditions at its opposite ends (or in the grating-gated FET structure with a symmetric unit cell) if there is no DC bias current flowing in the channel. In a periodic structure with a homogeneous 2D electron channel, the electron convection term in the Euler equation [the second term in Eq. (5)] does not contribute to the detection signal of the entire structure incorporating many dozens of periods because the spatial average of this term over the structure period is zero. Therefore, the only source of hydrodynamic nonlinearity in the periodic structure with a homogeneous 2D electron channel is the product $N(x,t)V(x,t)$ defining the current density in 2D electron fluid. However, if the equilibrium electron density in 2D channel varies over the structure period, the electron convection term in the Euler equation can vastly contribute to the detection signal.

In a FET with periodic grating gate, the DC photocurrent induced in 2D electron channel by incoming THz radiation can be calculated in the perturbation approach using the Fourier representation of Eqs. (5) and (6) [15]:

$$j_0=-e\sum_{q\neq 0}\left(N_q^{(0)}V_{0,-q}+N_{0,q}V_{-q}^{(0)}\right)- -2e\,\mathrm{Re}\sum_{q\neq 0}N_{\omega,q}V_{\omega,q}^{*}, \quad (7)$$

where $N_{\omega,q}$, $V_{\omega,q}$ and $N_{0,q}$ $V_{0,q}$ are the amplitudes of the space-time Fourier harmonics of the induced electron density and velocity at the frequency $\omega$ of incoming THz radiation and at zero frequency, respectively, and $N_q^{(0)}$ and $V_q^{(0)}$ are the amplitudes of the spatial Fourier harmonics of the equilibrium electron density $N^{(0)}(x)$ and DC drift velocity $V^{(0)}(x)$ in 2D electron channel (DC drift velocity is related to the equilibrium electron density as $V^{(0)}(x) = j_{bias}/eN^{(0)}(x)$ with $j_{bias}$ being the DC bias current density in 2D electron channel). It is worth noting that $N_{\omega,q}$ and $V_{\omega,q}$ are linear in the electric field amplitude of incoming THz wave, while $N_{0,q}$ and $V_{0,q}$ are proportional to the second power of the electric field amplitude of incoming THz wave in the perturbation approach.

The photocurrent given by Eq. (7) is zero in the grating-gate structure with a symmetrical unit cell when there is no DC electron drift in 2D electron channel. Therefore, THz photoresponse defined by Eq. (7) is exhibited in a symmetrical structure as the THz photoconductivity effect only when non-zero DC bias current is flowing in the 2D channel. In a 2D system with homogeneous electron density, only the second-sum term survives in the right-hand side of Eq. (7). This term describes the plasmon-driven DC electron drag in the 2D system because every $q$th summand in the series is proportional to the wave vector of the corresponding Fourier harmonic of the induced electric field in 2D channel [16]. [In a grating-gate structure with a symmetrical unit cell and without DC electron drift in 2D electron channel, the Fourier-harmonics of the electric field having the wave vectors of opposite signs have equal amplitudes and, hence, the net electron drag effect is zero]. The first-sum term in Eq. (7) is present only in 2D electron system with spatially modulated electron density. This term originates from the electron convection nonlinear term in the Euler equation Eq. (5). The photocurrent described by this term can be interpreted as a result of the plasma electrostriction effect in 2D electron system with inhomogeneous electron density [15] since the amplitudes of the space-time Fourier harmonics of the induced electron density and velocity at zero frequency entering the first-sum term in Eq. (7) are proportional to the square of the electric field amplitude of incoming THz wave.

In the fixed DC bias current regime used in experimental studies of the THz photoconductivity [17,18], the THz photoresponse manifests itself as an additional source-drain DC photovoltage $\delta U_0 = -j_0 D/\sigma_0$ where $D$ is the entire channel length and $\sigma_0$ is spatially averaged DC conductivity of the channel. Figure 4 demonstrates the calculated photoresponse of the grating-gated GaAs/AlGaAs FET structure with the following parameters: $D$ = 2 mm, $L$ = 4$\mu$m, the width of the grating-gate finger $l$ = 2$\mu$m, the distance between the grating gate and the 2D channel $d$ = 0.4$\mu$m, $j_{bias}$ = 0.05 A/m,

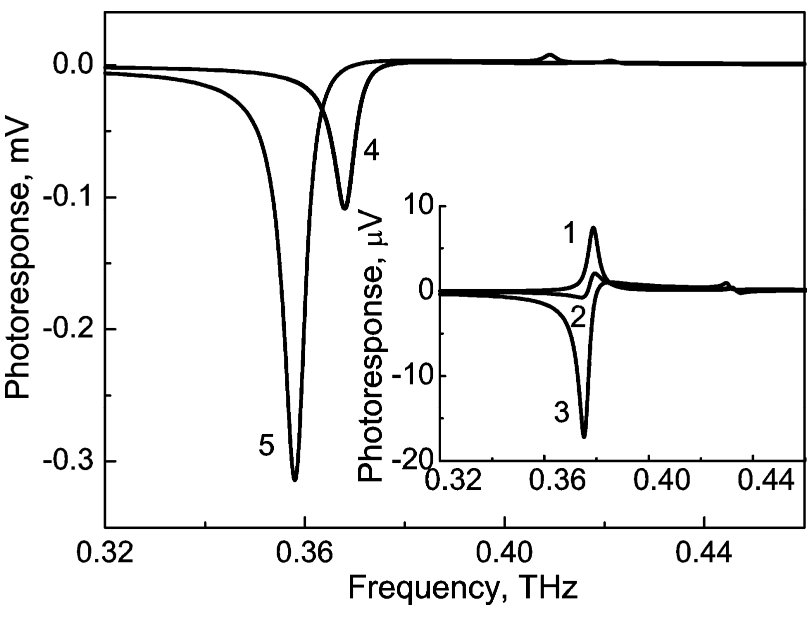


Fig. 4. Photoresponse vs frequency near the fundamental plasmon resonance for a density modulated grating-gated GaAs/AlGaAs FET structure at different values of the modulation factor α (see text): α=0 (curve 1), α=0.003 (curve 2), α=0.01 (curve 3), α=0.05 (curve 4), and α =0.1 (curve 5) [15]

the electron scattering time in 2D channel $\tau$ = 6.67×10$^{-11}$ s, and the input THz intensity 1W/cm$^2$. The photoresponse $\delta U_0$ is shown in Fig. 4 as a function of the THz frequency near the fundamental plasmon resonance at different values of the electron density modulation factor $\alpha = (N_2 - N_1)/(N_2 + N_1)$ for a sinusoidal profile for the equilibrium 2D electron density in 2D electron channel, where $N_2$ ($N_1$) is the maximum (minimum) value of the 2D electron density between the gate fingers (under the gate fingers). The photoresponse peak in Fig. 4 is the result of the resonant enhancement of the THz electric field in the 2D channel when the fundamental plasmon mode is excited in the 2D channel. The height of the peak strongly depends on the modulation factor. At $\alpha = 0$ the photoresponse is determined solely by the plasmon-driven electron drag [16]. The electron drag term practically does not depend on $\alpha$, whereas the electrostriction term vastly increases with in density modulated 2D electron channel.

**Conclusions**

Employing the plasmon excitations in FET structures with 2D electron channels can pave the way to designing electrically tunable THz microdevices in a broad THz range. Plasmonic nonlinear response is determined by the hydrodynamic nonlinearities of 2D electron fluid with plasmon velocity controlling the speed of the response. Since the plasmon velocity is, typically, by two orders of magnitude higher than the electron transfer velocity in 2D electron channel, the plasmonic devices can, potentially, be extremely fast.

**References**

1. *Dyakonov M. and Shur M.*, Detection, mixing, and frequency multiplication of terahertz radiation by two-dimensional electronic fluid // IEEE Trans. Electron Devices. 1996. V. 43. N. 3, P. 380-387.

2. *Knap W., Lusakowski J., Parenty T., Bollaert S., Cappy A., Popov V.V., Shur M.S.*, Terahertz emission by plasma waves in 60 nanometer gate high electron mobility transistors // Appl. Phys. Lett. 2004. V. 84, N. 13. P. 2331-2333.

3. *Coquillat D, Nadar S., Teppe T., Dyakonova N., Boubanga-Tombet S., Knap W., Nishimura T., Otsuji T., Meziani Y.M.,Tsymbalov G.M., Popov V.V.,* , Room temperature detection of sub-terahertz radiation in double-grating-gate transistors // Opt. Express. 2010. V. 18. P. 6024-6032.

4. *Marem'yanin K.M, Ermolaev D.M., Fateev D.V., Morozov S.V., Maleev N.A., Zemlyakov V.E., Gavrilenko V.I., Popov V.V., and Shapoval S.Yu.*, Wide-aperture detector of terahertz radiation based on GaAs/InGaAs transistor structure with large-area slit grating gate // Tech. Phys. Lett. 2010. V. 36, N. 4, P. 365–368 [Pis'ma v Zh. Tekh. Fiz. 2010. V. 36, N. 8, P. 39-47].

5. *Knap W., Dyakonov M., Coquillat D., Teppe F., Dyakonova N., Łusakowski J., Karpierz K., Sakowicz M., Valusis G, Seliuta D., Kasalynas I., El Fatimy A., Meziani Y.M., Otsuji T.*, Field effect transistors for terahertz detection: Physics and first imaging applications // J. Infrared Millim. Terahertz Waves. 2009. V. 30, N. 12, P. 1319-1337.

6. *Muravev V.M., Kukushkin I.V., Smet J., and von Klitzing K.*, Millimeter/submillimeter mixing based on the nonlinear plasmon response of two-dimensional electron systems // JETP Letters. 2009. V. 90. N. 3, P. 197–201 [Pis'ma v Zh. Eksper. Teor. Fiz. 2009. V. 90. N. 3. P. 216-221].

7. *Chaplik A.V.*, Possible crystallization of charge carriers in inversion layers with low density // Sov. Phys. JETP. 1972. V. 35, P. 395-402 [Zh. Eksp. Teor. Fiz. 1972. V. 62, N. 2, P. 746-753].

8. *Dyakonov M. and Shur M.*, Shallow water analogy for a ballistic field effect transistor: new mechanism of plasma waves generation by dc current // Phys. Rev. Lett. 1993. V. 71. N. 15, P. 2465-2468.

9. *Ritchie R.H.*, Plasma losses by fast electrons in thin films // Phys. Rev. 1957. V. 106. N. 5. P. 874-881.

10. *Stern F.*, Polarizability of a two-dimensional electron gas // Phys. Rev. Lett. 1967. V. 18. N. 14. P. 546-548.

11. *Dyakonov M. and Shur M.S.*, Current instability and plasma waves generation in ungated two-dimensional electron layers // Appl. Phys. Lett. 2005. V. 87. N. 11. P. 111501 (3 p.).

12. *Popov VV., Polischuk O.V., Shur M.S.*, Resonant excitation of plasma oscillations in a

partially gated two-dimensional electron layer // J. Appl. Phys. 2005. V. 98. N. 3. P. 033510 (7 p.).

13. *Theis T.N.*, Plasmons in inversion layers // *Surface Science*. 1980. V. 98. P. 515-532.

14. *Popov V.V., Shur M.S., Tsymbalov G.M., Fateev D.V.*, Higher-order plasmon resonances in GaN-based field-effect transistor arrays // Int. J. High Speed Electronics and Systems. 2007 V. 17. N. 3, P. 557-566.

15. *Aizin G.M., Fateev D.V., Tsymbalov G.M., Popov V.V.*, Terahertz plasmon photoresponse in a density modulated two-dimensional electron channel of a GaAs/AlGaAs field-effect transistor // Appl. Phys. Lett. 2007. V. 91. N. 16. P. 163507 (3 p.).

16. *Aizin G.R., Popov V.V., Polischuk O.V.*, Plasmon enhanced electron drag and terahertz photoconductance in a grating-gated field-effect transistor with two-dimensional electron channel // Appl. Phys. Lett. 2006. V. 89. N. 14. P. 143512 (3 p.).

17. *Peralta X.G., Allen S.J., Wanke M.C., Harff N.B., Simmons J.A., Lilly M.P., Reno J.A., Burke P.J., and Eisenstein J.P.*, Terahertz photoconductivity and plasmon modes in double-quantum-well field-effect transistors // Appl. Phys. Lett. 2002. V. 81. N. 9. P. 1627-1629.

18. *Shaner E.A., Lee Mark, Wanke M.C., Grine A.D., Ren J.L., and Allen S.J.*, Single-quantum-well grating-gated terahertz plasmon detectors // Appl. Phys. Lett. 2005. V. 87. N. 19. P. 193507 (3 p.).

*22.09.2010*